

DETECTION OF LUMEN-INTIMA INTERFACE MOTION OF PERIPHERAL ARTERY FOR MEASUREMENT OF ELASTICITY PROFILE

O. Laouini¹, F. Essafi¹, L.Bressollette², E.Ben Braiek³

¹Faculty of Medicine of Tunis, Department of Biophysics Tunis, University Tunis El Manar.

olfa.laouini@gmail.com

²University Hospital of Brest, Unit Vascular Echo-Doppler Device And Vascular Medicine CHU La Cavale Blanche

³Higher National School of Engineers of Tunis, Research Center of Productics CEREP , Group on Vision and Image Processing

ABSTRACT

The parameters associated with vessel wall elasticity are of particular interest since they offer a possibility to separate diseased and healthy arteries. The physical and biological factors inducing the decrease of vessel wall elasticity aren't well known. Studying the elastical properties of peripheral arteries could help us to identify some of these physical parameters. Performing a non-invasive measurement of such parameters is quite difficult. Therefore, in vivo ultrasonic measurement systems, such as the Doppler ultrasound imaging were utilized. Methods adopted were based on measurement of ultrasonic elasticity of peripheral arteries and evaluation of deformation with vessel wall pressure. The proceeding of obtained ultrasonic B-mode images consists in Semi-Automated Endoluminal Contour Detection using sveral active contour segmentation methods and geometrical measurements in order to evaluate the shear stress, elastic modulus and the compliance of peripheral arteries. Results for these parameters revealed a new technique to study the decrease of vessel wall elasticity.

Keywords: Semi-automatic image processing, active contour, ultrasound imaging, arterial wall, shear stress, elastic modulus, compliance.

1 INTRODUCTION

Vascular Ultrasound imaging is an in-development non-invasive imaging technique, which estimates the arterial wall deformation during a cardiac cycle. This technique aims of the accurate depiction of the elastical properties of the peripheral arterial wall, and thus might provide useful information to detect abnormalities and to predict the disease evolution. Edge detection of arteries is generally indispensable for practitioners, in order to investigate the evolution of these contours for purpose of diagnostic aid.

Until now, Doctors often use manual segmentation methods to detect deformations in arterial walls caused by elasticity decreasing.

More and more specialist desired to have a simple manipulation platform with a short calculation time. Which results could be used for later quantitative studies in order to determinate certain physical parameters of peripheral arteries.

The automation of this process is desirable were segmentation is performed in minutes by the specialist.

However, the nature of ultrasound images makes it a little tricky task.

Considering a priori knowledge provided by the expert and geometric properties of the arterial wall, we were interested to study and combine two simple and fast methods.

The first method demonstrate the segmentation based on the active contours Chan-Vese [2].

The second type used the Chan and Vese model based on the topological derivative [3].

2 MATERIALS AND METHODS

2.1 ULTRASOUND MEASUREMENTS

The humeral arterial wall systolic-diastolic motion was estimated using the Doppler – echography and a high frequency linear probe of 12 MHz. All cross-sectional

ultrasound images are detected applying the duplex technique associated with electro-cardio-gram (ECG).

2.2 FORMULATION OF ELASTICAL PARAMETERS

The different shear stresses are based on the systolic-diastolic variation of intraluminal radius R , of the first cross-sectional image 0 and the last cross-section i of the artery.

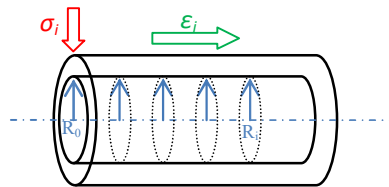


Figura 1 - Fig.1 Illustration of arterial wall longitudinal and transversal shear stress locations

The longitudinal shear stress ϵ_i , during the systolic-diastolic transition, which applies on the side surface of the artery (Figure 1) is given by equation (1):

$$\epsilon_i = \frac{R_i - R_0}{R_0} \quad (1)$$

TRANSVERSAL SHEAR STRESS

The transversal shear stress is applied on the transversal surface of the artery (Figure 1). It is given in (equation (2)):

$$\sigma_i = \frac{R_i^2 - R_0^2}{R_0^2} \quad (2)$$

We define two vectors one systolic and second diastolic, respectively by the matrixes $\{\epsilon_1, \sigma_1, P_1\}$ and $\{\epsilon_2, \sigma_2, P_2\}$. Given the variation of the blood pressure of the diastole (1) and systole (2) phase, we propose to calculate the elasticity modulus E_i (Young's modulus) and the compliance C_i of the arterial wall using the formulas below.

YOUNG MODULUS

$$E_i = \frac{P_2 - P_1}{\varepsilon_2 - \varepsilon_1} \quad (3)$$

ELASTIC COMPLIANCE

$$C_i = \frac{\sigma_2 - \sigma_1}{P_2 - P_1} \quad (4)$$

2.3 DATA IMAGE PROCESSING TECHNIQUE

The area of interest is the endoluminal peripheral artery section it's magnitude is about millimeters so all our segmentation are realized without preprocessing the ultrasound images, in order to preserve all diagnostic information. Our acquisition method detects five successive frames on the same artery. This method requires the intervention of an expert with the intention of delimitating the area of interest on the first frame, so we are challenged with a volume of ultrasound data.

2.3.1 CHAN AND VESE MODEL

Detecting the arterial wall contour in ultrasound images is very tricky task especially if we want a solid final result. Dividing our images in to two or more areas, like regions of interest and background is very helpful so we're interested in the region-based active contours model [3].

This model [4] tries to stop the evolution of the curve with an energy minimization approach rather than using an edge-stopping function. Considering a simple case where the image u_0 is formed by two regions of piecewise constant intensity. The proposed energy function is as below:

$$E(\gamma, c_1, c_2) = \mu \cdot \text{Lenght}(\gamma) + \nu \cdot \text{Area}(\text{inside}(\gamma)) + \lambda_1 \cdot \int_{\text{inside} \gamma} |u_0(x, y) - c_1|^2 dx dy + \lambda_2 \cdot \int_{\text{outside} \gamma} |u_0(x, y) - c_2|^2 dx dy, \quad (5)$$

Where $\mu, \nu \geq 0$ and $\lambda_1, \lambda_2 > 0$ are fixed parameters.

The two real c_1 and c_2 are respectively the averages of grey level intensities inside and outside γ . The first two terms help the curve to be regular, and the two others correspond to the energy inside and outside the curve. The minimum of the previous energy is obtained when the curve is on the boundaries of the object to be detected. This energy can be formulated using level set methods: the evolving curve γ can be represented by the zero level set of a signed function Φ , ($z = \Phi(x, y)$). Now consider the Heaviside function H , and the Dirac measure δ . If we consider z as a level of Φ we're able to write:

$$H(z) = \begin{cases} 1, & \text{if } z \geq 0 \\ 0, & \text{if } z < 0 \end{cases}, \delta(z) = \frac{dH(z)}{dz},$$

Let Ω be the image domain, then the area of the region inside the curve is just the integral of the Heaviside function of $-\Phi$. The gradient of the Heaviside function defines the curve, so integrating over this region gives the length of the contour as below.

$$Area(\Phi = 0) = \int_{\Omega} H(-\Phi(x, y)) dx dy$$

$$Length(\Phi = 0) = \int_{\Omega} \delta(\Phi) |\nabla \Phi(x, y)| dx dy$$

Therefore the energy function $E(\gamma, c_1, c_2)$ can be written as

$$\begin{aligned} E(\gamma, c_1, c_2) &= \mu \cdot \int_{\Omega} \delta(\Phi) |\nabla \Phi(x, y)| dx dy + \\ &+ \nu \cdot \int_{\Omega} H(-\Phi(x, y)) dx dy + \lambda_1 \cdot \int_{\Omega} |u_0(x, y) - c_1|^2 H(-\Phi(x, y)) dx dy \\ &+ \lambda_2 \cdot \int_{\Omega} |u_0(x, y) - c_2|^2 H(\Phi(x, y)) dx dy, \end{aligned} \quad (6)$$

Where c_1 and c_2 are computed as

$$c_1 = \frac{\int_{\Omega} u_0(x, y) \cdot H(-\Phi(x, y)) dx dy}{\int_{\Omega} H(-\Phi(x, y)) dx dy},$$

$$c_2 = \frac{\int_{\Omega} u_0(x, y) \cdot H(\Phi(x, y)) dx dy}{\int_{\Omega} H(\Phi(x, y)) dx dy},$$

The discrete and linear involving equation obtained in the Euler-Lagrange framework by estimating the curvature $K_{i,j}$ from $\Phi_{i,j}^n$ is:

$$\frac{\Phi_{i,j}^{n+1} - \Phi_{i,j}^n}{\Delta t} = \delta_{\varepsilon}(\Phi_{i,j}^n) \left(-\mu \cdot K_{i,j} + \nu + \lambda_1 \cdot |u_0^{i,j} - c_1|^2 - \lambda_2 \cdot |u_0^{i,j} - c_2|^2 \right),$$

Where $\delta_{\varepsilon}(z)$ is a regular form of $\delta(z)$ proposed in [3].

APPLICATION OF THE CHAN –VESE MODEL

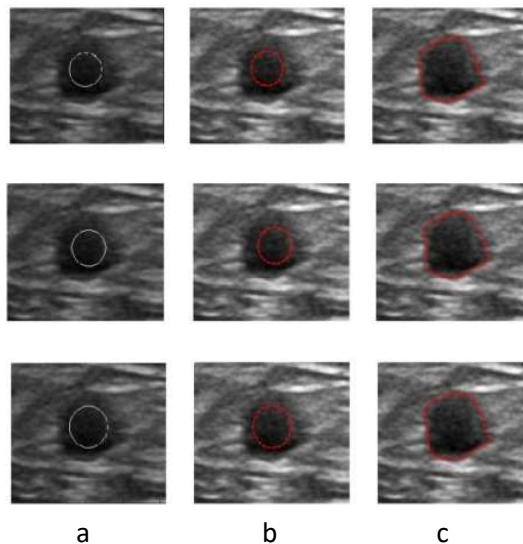


Figure 2 - Chan-Vese method application on the same frame (diastolic phase) : in (a), region of interest selection: original Image, (b) : algorithm initialization deformation of the contour, (c) : final shape of the contour, (personnel Images)

We note that Figure 3 shows that the contours vary for the same artery and the same frame and in the same phase (diastole). It is characterized by the initialization problem [3]. According to the statistical calculations (Test student) of our studied subjects using SPSS 20 we only detect 62% of the endoluminal arterial wall. Furthermore, the calculation errors of the physical parameters, based on this model were statistically significant ($> 5\%$). This leads us to think of a more appropriate method for our purposes of calculating physical parameters of the artery.

2.3.2 CHAN-VESEMODEL BASED ON THE TOPOLOGICAL DERIVATIVE

In image segmentation, the topological derivative is used to solve the problem of energy functional minimization equation (6) of the model (CV) in the case of two-phase and multiphase.

Constants λ_k in the equation is taken equal to 1. Some authors, attempt to simplify the expression (6), considering $\mu = 0$. They advocate in the case of a noisy image, either to apply their algorithms to a nonlinear diffusion filtered image, to approximate the term

$\int_{\Omega} |\nabla H(\Phi)| dx dy$ [4,5,6,7], by the expression:

$$\sum_{i,j} \sqrt{(H(\Phi_{i+1,j}) - H(\Phi_{i,j}))^2 + (H(\Phi_{i,j+1}) - H(\Phi_{i,j}))^2} \quad (7)$$

Where $\Phi_{i,j}$ is the Φ value on the pixel level (i, j) . Noting that the term under the square root can take only the values 0, 1 or 2 depending on whether the corresponding points of the three pairs of ensemble elements $\{\Phi_{i,j}, \Phi_{i+1,j}, \Phi_{i,j+1}\}$ belong or not to the same region.

APPLICATION OF (CV) BASEDON TOPOLOGIC DERIVATIVE: MONOPHASIC IMAGES (GREY SCALED)

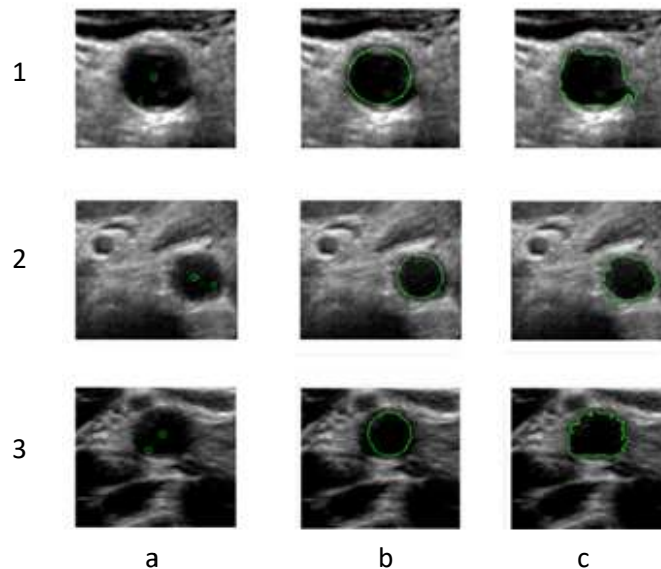


Figure 3 - Chan-Vese based topologic derivative method application on the same frame (diastolic phase) : in (a), points selection on region of interest : original Image, (b) : algorithm initialization contour deformation, (c) : final shape of the contour, (personnel Images)

APPLICATION OF (CV) BASED ON TOPOLOGIC DERIVATIVE: THE MULTIPHASIC IMAGES

Remind that the Doppler images are multi-spectral images. They're result is the superposition of a grayscale image (ultrasound) with a RGB image representing the color code of the Doppler flow distribution in the artery. The numerical size of Doppler images is represented by a third order matrix. This matrix and shows the three layers background, image region of interest and Doppler color code.

In order to detect the arterial wall contour in this case it is necessary to break the image (I) into two layers with an algorithm that will ensure the respective boundaries of the image in grayscale with the background (J1) and the image in RGB (J2) (Figure 5 (a)).

To isolate the color part of image (J2) means to get rid of the residuals noisy background (speckle). To do this, we applied a mathematical morphology mask, structuring element of "ellipse" on the image (J2) (Figure 5 (1-4b)).

Finally, we end with the implementation of the active contour algorithm of Chan-Vese based on topology derivative, in order to extract the arterial wall lumen (Figure 5 (1-4c)).

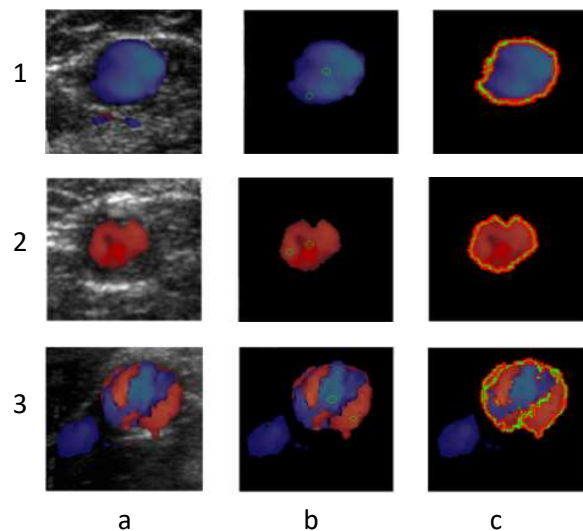


Figure 4 - Chan-Vese based topologic derivative method application on the different frames (diastolic phase) : in (1-3b), points selection on region of interest : original Images, (1-3c) : final shape of the contour, (personnel Images)

Our results on multiphase Doppler ultrasound images are generally acceptable. However, this semi-automatic preprocessing which goes from images (a) to images (b) is very tricky because it requires at each time a re-initialization of the morphological mask.

Therefore, this is an operator-dependent process and requires additional processing time.

Moreover, the Doppler images are very multi-operator dependent. To avoid such problems, it is necessary that the ultrasound system is properly calibrated especially at the focus and intensity of the Doppler signal.

Otherwise (Figure 5 (3c)), the Doppler signal can exit the region of interest (detecting a vein signal besides the arterial lumen). According to the statistical calculations (Test

student) of our studied subjects using SPSS 20 we detect 98% of the endoluminal arterial wall. At this time the detected contour is performed in a located area outside of the region of interest, so the error of determining the elastical parameters of the arterial wall will generate much more than 5%.

2.4 NUMERICAL CALCULATIONS

In order to perform numerical calculations of the elastic parameters of the arterial wall, we added features to this algorithm that we previously developed to describe the geometric model that we have adopted to determine the systolic and diastolic phase of the artery.

2.4.1 ALGORITHM MEASURING CONTRACTION OF THE ARTERIAL WALL DURING THE SYSTOLE-DIASTOLE TRANSITION CENTROID OF THE ARTERIAL LUMEN

In order to determine the geometric parameters of the arterial contour, we have determined a common center point “centroid” for each sequence of the binarized cross-sectional frames.

Indeed, the calculations of the arterial elastic properties is closely linked to variations of the arterial wall contour that we have materialized in different points of the contour by the polar coordinates (r, Θ) .

The detailed study of the artery edge requires a single reference point, preferably for all obtained images a central point located inside the edge.

To do this, we determined the centroid of a sequence of cross-sectional images of non-smokers. The same center was considered for smoker about the same age and for both systolic and diastolic image. This allowed us to compare the processed images for same aged smokers and non-smokers.

The calculation of the centroid is based on the Euclidean distance using the equation $d(r, s) = \|\bar{x}_r - \bar{x}_s\|_2$, where $\bar{x}_r = \frac{1}{n_r} \sum_{i=1}^n x_{r_i}$.

2.4.2 ARTERIAL ENDOLUMINAL RADIUS VARIATIONS MEASUREMENTS

The endoluminal radius variations, allows us to study the arterial wall elastic properties. For this it's sufficient to analyze the variation of the inner arterial wall radius r function the positioning angle Θ . Our "signature" process is function of a one-dimensional the segmented contour. Based on the assumption of a uniform scale respecting the two axes of the bi-dimensional reference the radius r and the position angle Θ are measured by considering equal intervals. It's possible and even necessary to use not two, but four axes and sometimes even eight ($2^1, 2^2, 2^3$), it's depending on the shape of the frame. More the shapes are distorted more it is desirable to use multiple axes. Variations in the size and shape of the analyzed contour result the corresponding amplitudes values function.

In addition, the signature depends on whether the image is in the systolic or diastolic phase (Figure 5).

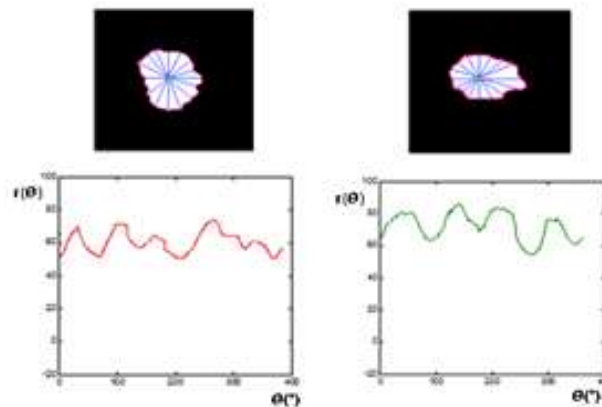


Figure 5 - Endoluminal radius variation function θ (diastolic on the right systolic on the left)

The advantage of our method is the simplicity, but the potential downside is that the scale of this function is based on just two values of the distance from the adopted centroid: maximum distance and minimum distance around the centroid. These algorithms, fast, have been mainly developed for the two-phase model. An extended method multiphase model was proposed but it multiphase model is limited to images

made up of four regions. This implies that only uses one or two level set functions. In addition, construction areas is complex because it is performed by combinations of several level set functions.

In our work, Doppler color images never contain more than four regions (colors) and this problem does not arise.

3 RESULTS AND DISCUSSIONS

The validation of our model first requires a study of a group of 35 healthy subjects. We detected Doppler-ultrasound images of the humeral artery using the previously mentioned method. Figure 9 shows the variations of the endoluminal radius function the position angle Θ , of the humeral artery during the systolic and diastolic phase, at one cardiac cycle.

In systole: Figure (9-a): The variation of the humeral endoluminal artery radius depends on the angle position Θ and remains a low average value (2.01 ± 0.01) mm

In diastole: Figure (9-b): The variation of radius shows a more rugged look with a mean value of (2.41 ± 0.07) mm.

- (a): Endoluminal radius R_1 variation at systolic phase.
- (b): Endoluminal radius R_2 variation at diastolic phase.
- (c): Radius "GAP" variation : $R_2 - R_1$.

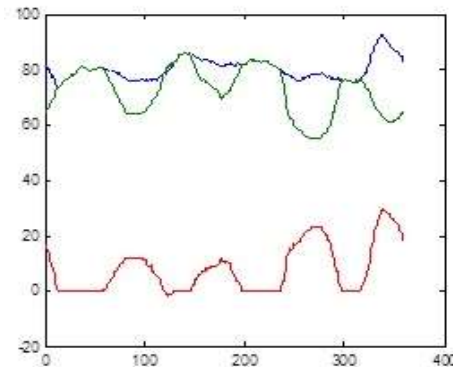


Figure 6 – Humeral endoluminal radius R_i (vertical) variation function angle position θ (horizontal)

Curve (9-c) shows the variation of the radius 'GAP' ($R_2 - R_1$) based Θ . It clearly indicates that the arterial wall is more deformed during the diastolic phase than the

systolic phase. The GAP mean value is about (0.50 ± 0.037) mm. This given result in the humeral artery is confirmed for all the variations of the endoluminal radius of all our studied subjects. The variations of Young's modulus E_i and elastic compliance C_i of the arterial wall contraction during systole-diastole transition at one cardiac cycle.

Table 1: Mean values of geometric and elastic parameters in humeral artery

Humeral artery	Systolic Radius (mm)	Diastolic Radius (mm)	Radius GAP (mm)	Young Modulus (mmHg)	Elastic Compliance (mmHg⁻¹)
Mean Value	2.01	2.41	0.50	244.07	0.580
Std. Error Mean value	±0.01	±0.07	±0.037	±33.38	±0.037

The important capacitive effect of the humeral artery is due to the proximity of this artery to the heart. This effect will give the possibility of the humeral artery to open and close more than other peripheral arteries during to the gap it could be e up to 2.6 mm ($0 < (R_2 - R_1) \leq 2,6\text{mm}$). The average values of the elastic compliance shows a significant variation during diastole-systole transition, which is explained by the fact that the diastolic phase keeps the arterial wall in an elastic relaxation.

Moreover, we note a sensitivity of the longitudinal and transversal shear stress with a significant change of the Young modulus E_i and compliance C_i of the artery. Another histological factor could have an influence on the results.

Indeed, it is well known that elastin fibers are more elastic than collagen fibers. Furthermore, in histological sections of the peripheral arterial wall, the elastin fibers are below the collagen fibers. This shows that the transversal shear stress is stronger than the longitudinal shear stress. In other words the artery inflates more than it lain. It is

well known as the capacitive effect of the arteries. This result confirms the relationships in equations (1) and (2).

4 CONCLUSION

After the digital image and signals processing, we can conclude that arterial Doppler ultrasound imaging system is used to enter the ultrasonic elasticity of peripheral arteries and assess the state of the pressure and the magnitude of the arterial wall deformation.

Thus, we have developed and used a digital method to develop a platform in order to determinate the physical parameters of the arteries.

We therefore find that it's possible to observe and quantify the state of the peripheral arteries elasticity using a noninvasive method consisting of a Doppler-ultrasound imaging followed by digital image processing.

We intend, through this interface, for our future studies to work on diabetes, calcification of the mitral valves, arterial prostheses engineering...

This study could be extended by a working simulation that would be performed on phantoms made in vascular prostheses materials.

We hope to create anelastic profiles reconstruction software of arterials Doppler-ultrasound images and thus to serve directly or indirectly in peripheral vascular prostheses engineering.

5 REFERENCES

- [1] T.Chan and L. Vese, "Active contours without edges," IEEE Trans. Imag.Proc., vol. 10, pp. 266-277, 2001
- [2] V. Caselles and J. Morel, Introduction to special issue on partial differential equations and geometry-driven diffusion in image processing and analysis, IEEE Trans. On Image Processing, volume 7(3) pages 269-273, 1998.

SCIENTIFIC SOCIETY

MULTIDISCIPLINAR MAGAZINE

VOLUME 1, NÚMERO 2, NOVIEMBRE DE 2018

ISSN: 2595-8402

DOI: 10.5281/zenodo.1567203

- [3] T. McInerney and D. Terzopoulos, Deformable models in medical image analysis: a survey, in Medical Image Analysis, volume 1(2) pages 91-108, 1996.
- [4] Pietro Perona and Jitendra Malik, Scale-Space and Edge Detection Using Anisotropic Diffusion, IEEE transactions on pattern analysis and machine intelligence, volume 12. No.7. July 1990
- [5] M. Black, G. Sapiro, D. Marimont, and D. Heeger, Robust anisotropic diffusion and sharpening of scalar and vector images, IEEE Intern. Conf. on Image Processing, Volume 2 pages 1001-1006, Oct 1997.
- [6] P. Perona. Orientation diffusions. IEEE Trans. on Image Processing, volume 7(3) pages 457-467, 1998
- [7] J. Weickert, B.M. Romeny and M.A. Viergever, Efficient and reliable schemes for Non-linear diffusion filtering. IEEE Trans. on Image Processing, volume 7(3) pages 398-410, 1998.